Article

Not peer-reviewed version

Geochemistry of Cenozoic Basaltic Rocks from Anhui Province, China: Implications for Their Petrogenesis and Mantle Processes

Yung-Tan Lee * and Meng-Lung Lin

Posted Date: 15 November 2023

doi: 10.20944/preprints202311.0972.v1

Keywords: Anhui province; petrogenesis; mantle processes; metasomatism

Article

Geochemistry of Cenozoic Basaltic Rocks from Anhui Province, China: Implications for Their Petrogenesis and Mantle Processes

Yung-Tan Lee [1,*] and Meng-Lung Lin [2]

[1] Department of Tourism and Travel Management, Taipei University of Marine Technology, New Taipei City, Taiwan, ROC ; yungtan@mail.tumt.edu.tw
[2] Department of Tourism, Aletheia University, New Taipei City, Taiwan, ROC; mllin1976@mail.au.edu.tw
* Correspondence: yungtan@mail.tumt.edu.tw; Tel.:+886-2-28059999 Ext. 5120

Abstract: Based on the major, trace element, and isotope data of the Cenozoic basalts in the study area, it is indicated that the basalts in this region can be classified into three distinct magma systems: alkali basalts, tholeiite basalts, and Nushan alkali basalts. The geochemical characteristics observed in the studied basalts indicate that the mantle source in this region might have experienced metasomatic processes prior to partial melting, which could be linked to an ancient subduction process. Combining the geochemical characteristics in the studied basalts with previous research, we propose that the underlying mantle source in Anhui province may have undergone metasomatism due to the carbonatitic melts. These melts are believed to have originated from carbonated eclogite, derived from subducted Pacific slab materials present in the deeper mantle. According to the Sr-Nd isotope data, it is suggested that the mantle source in the Nushan region could be derived from a depleted asthenospheric mantle, while the basaltic composition in the Niugang area may be representative of the mantle's end components associated with the EM-I enriched mantle source present in this study area. Therefore, we propose that the Anhui basalts may have originated from the partial melting of a mantle source representing a mixing of two end-members: DMM (Depleted MORB Mantle) and EM-I (Enriched Mantle 1). The Anhui basaltic magmas may have originated from the partial melting of EM-I, potentially influenced by upwelling asthenospheric mantle or asthenospheric diapirism processes. The mantle source in the study area experiences partial melting at 1-5%, 15%, and 1-10%, resulting in the formation of parent magmas for alkali basalt, tholeiitic basalt, and Nushan alkali basalt. Subsequently, the parent magmas experienced fractional crystallization processes, which included minerals like olivine, pyroxene, and plagioclase. This led to the formation of various types of basalt in the study area.

Keywords: Anhui province; petrogenesis; mantle processes; metasomatism

1. Introduction

Anhui Province's basalt formations are located at the intersection of the Yangtze Craton's boundary and the southeastern edge of the Sino-Korean Craton, which is renowned as one of the most ancient Archean continental nuclei globally [1–3]. Stretching across more than 4000 kilometers from Siberia to Eastern China, there exist Cenozoic extensional basins and concurrent volcanic eruptions along the continental margin of eastern Asia. Cenozoic basalt formations exhibit extensive distribution, spanning from the northern reaches of Heilongjiang province to the southern expanse of Hainan Island and the South China Sea [4]. The Cenozoic volcanic rock formations within the Anhui-Jiangsu provinces cover an expansive region exceeding 2,000 km^2 in Eastern Anhui and Western Jiangsu. The spatial arrangement of volcanic rock formations within Anhui-Jiangsu provinces is influenced by the NNE-trending Tan-Lu fault, which originated due to lithospheric extension.

Over the past few years, a number of researchers [5–8] have advanced the idea that the North China Craton (NCC) might have experienced lithospheric thinning since the Palaeozoic era, possibly as a consequence of the physical disruption of the craton resulting from the Triassic collision between the NCC and the Yangtze Block. Sun et al. (2021) [9] concluded that the lithosphere thinning in eastern continental China since the Mesozoic is a straightforward consequence of plate tectonics. The lithosphere thinning in the Mesozoic resulted from basal hydration weakening with the water coming from dehydration of the paleo-Pacific plate in the mantle transition zone. The weakening effect is to convert the basal lithosphere into asthenosphere by reducing its viscosity, having thus thinned the lithosphere while triggering mantle melting and crustal magmatism marked by the widespread Mesozoic basalts and granitoids in space and time. The lithospheric mantle found in the western portion of the Sino-Korean Craton (SKC) exhibits relatively greater age in contrast to the eastern SKC, which is posited to consist of a blend of older lithospheric remnants and newly accreted mantle [7]. There are still some disputes and unclear areas regarding the rock genesis and geodynamic background of the eastern continental region, which require further research and exploration. The exact mechanisms and timing of lithosphere thinning and magmatism in eastern China are still under debate. The aim of this paper is to conduct a comprehensive analysis of both major and trace elements, including rare-earth elements, and Sr-Nd isotopic ratios. Additionally, we will employ the Ar-Ar dating method to determine the ages of the basaltic rock. Through these investigations, we seek to infer the petrogenesis and magmatic evolution of these rock formations. Furthermore, we intend to elucidate the processes of differentiation that have influenced the chemical variations in these basaltic rocks. Lastly, our study aims to identify the geochemical attributes of the upper mantle beneath Anhui province.

2. Analytical Methods

In this research, we examined 23 Cenozoic basalts collected from Anhui province (as illustrated in Figure 1) through a comprehensive analysis of their bulk chemical composition. The major elemental constituents, including SiO_2, TiO_2, Al_2O_3, Fe_2O_3, MnO, MgO, CaO, Na_2O, K_2O, and P_2O_5, were quantified using an Energy Dispersive X-ray Fluorescence Spectrometer (EDX-900HS) at Chinese Culture University. To analyze all other trace elements (Ba, Co, Cr, Cs, Cu, Hf, Li, Nb, Ni, Rb, Sc, Sr, Ta, Th, U, V, Y, Zn, Zr, and Rare Earth Elements), rock powder samples were processed by dissolving 0.5 grams of material in a blend of ultrapure HF and HNO_3, within Teflon containers, under clean room conditions. The subsequent chemical assessments of these basalts were carried out using inductively coupled plasma mass spectrometry at Tsing-Hua University.

We chose five specific basalts (AG4, AB3, AL2, AN2, and AM2) to investigate their Sr and Nd isotopic compositions. The Sr and Nd isotopic compositions were determined by utilizing a Finnigan MAT 262 mass spectrometer located at National Cheng Kung University, following the protocols outlined by Smith and Huang (1997) [10].

The ages of five representative basalts (AG4, AB3, AL2, AS1, and AM2) were determined using the Ar-Ar dating method. A 40–120-mesh sieve-sized fraction of each sample, weighing approximately 1.5 to 3 grams, was carefully selected. Subsequently, these samples were securely enclosed in aluminum foil packets and arranged within an aluminum canister alongside LP-6 biotite (with an age of 127.7 ± 1.4 million years, as documented by Odin in 1982) [11] and HDB-1 hornblende (with an age of 24.7 ± 0.4 million years, based on Fuhrmann et al. in 1987) [12]. The canister, along with the standards and samples, underwent irradiation using fast neutrons within the VT-C position of the Open Pool Reactor at Tsing-Hua University. The neutron flux during irradiation was maintained at 1.566×10^{13} neutron/cm^2/sec for a duration of 8 hours. Following irradiation, the samples were loaded into degassed fused silica boats, allowed to cool for a minimum of two weeks, and then inserted into a degassed fused quartz tube. This quartz tube was subsequently heated at 250°C for 24 hours and subjected to incremental heating in accordance with a 30-minute per step schedule, utilizing a resistance furnace. The gas released during this process was purified and subsequently analyzed using a Varian-MAT GD 150 mass spectrometer.

3. Results

The surface appearance of the tholeiite basalts in this study is typically light gray or grayish. These rocks are characterized by a vesicular texture and often exhibit a porphyritic structure, with predominant phenocrysts of plagioclase and clinopyroxene. The matrix primarily consists of

Preprints (www.preprints.org) | NOT PEER-REVIEWED | Posted: 15 November 2023 doi:10.20944/preprints202311.0972.v1

plagioclase, pyroxene, magnetite, and a minor amount of glassy material. Alkali basalts typically exhibit a dark gray to deep black external appearance, with a predominance of blocky and vesicular textures in the rock. In certain areas, such as the Nu Shan region, some basalts display a minor porphyritic structure with predominant phenocrysts of olivine and titanium-rich augite, while the matrix mainly consists of plagioclase, pyroxene, olivine, and magnetite. We employed the Ne-Ol-Di-Hy-Qz tetrahedron introduced by Yoder and Tilley in 1962 [13] to categorize the basaltic rocks in this study into two types: tholeiite basalts and alkali basalt (Figure 2).

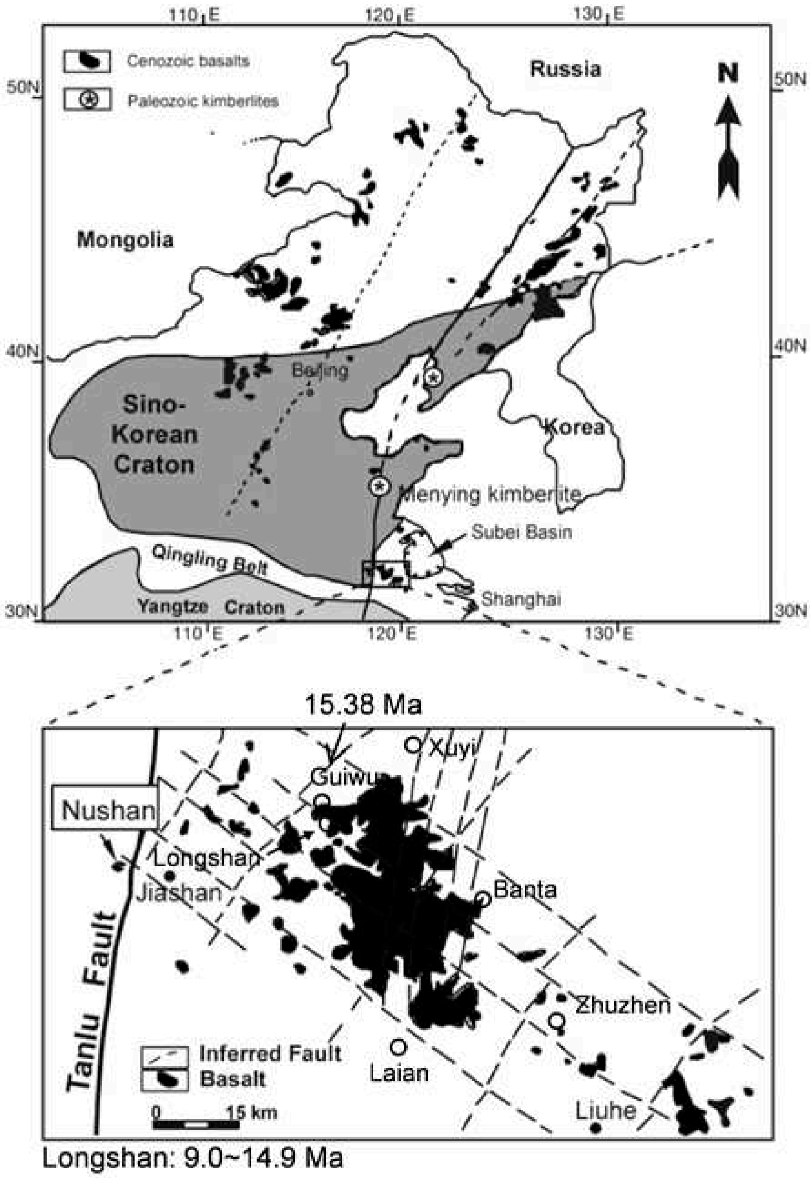

Figure 1. A simplified tectonic framework of eastern China and the specific study area's position are illustrated in a sketch map, with modifications from Xu and Bodinier (2004)[14].

Preprints (www.preprints.org) | NOT PEER-REVIEWED | Posted: 15 November 2023 doi:10.20944/preprints202311.0972.v1

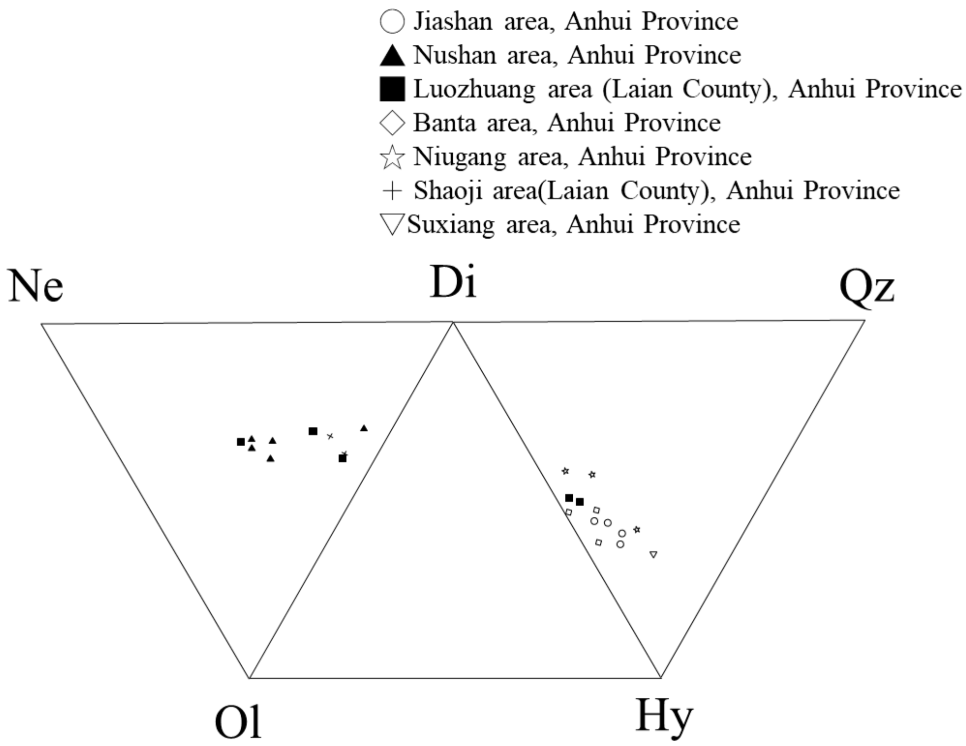

Figure 2. The normative compositions of basaltic rocks originating from Anhui province, following the volcanic rock nomenclature established by Yoder and Tilley in 1962 [13].

3.1. Major element geochemistry

The Table 1 displays the major element compositions and CIPW norms of basaltic rocks from Anhui province. In the study area, the SiO_2 content of alkali basalts ranges from 44.25% to 48.51% (with an average of 46.64%), while that of tholeiite basalts falls between 50.21% and 53.28% (with an average of 51.90%). There is a significant difference in SiO_2 content between these two types of basalts. Table 1 reveals differences in the major elements of alkali basalts and tholeiite basalts from the study area. We believe that there may be two possible reasons for these differences: (1) Alkali basalts and tholeiite basalts from the study area may originate from the same magma system: Alkali basalts may have formed from partial melting of the mantle source, followed by fractional crystallization processes involving minerals such as olivine, pyroxene, or plagioclase, ultimately evolving into tholeiite basalts; (2) Alkali basalts and tholeiite basalts within the study area may originate from different magma systems: Alkali basalts and tholeiite basalts may derived from the same mantle source, but their respective parent magmas may have formed through different degrees of partial melting. Due to the absence of olivine tholeiite in the sampled basaltic rocks in this study, we suggest that alkali basalts and tholeiite basalts may originate from two distinct magma systems.

Table 1. Major element compositions and CIPW norms of basaltic rocks from Anhui province.

Location	**Jiashan area**				**Nushan area**			
Sample	AG1	AG2	AG3	AG4	AM1	AM2	AM3	AM4
Rock type	TB	TB	TB	TB	AB	AB	AB	AB
SiO_2(wt%)	52.54	51.89	52.23	52.52	46.78	47.35	48.51	46.22
Al_2O_3	14.55	14.57	14.42	14.56	13.11	13.08	12.45	13.63
ΣFeO	10.50	10.40	10.19	10.15	11.42	11.35	10.92	11.35
MgO	6.92	7.05	6.98	7.19	8.01	8.24	6.75	8.00
CaO	8.40	9.20	8.87	8.11	7.70	6.95	9.89	6.74
Na_2O	2.75	2.87	2.78	2.91	6.02	5.89	3.82	5.08

Preprints (www.preprints.org) | NOT PEER-REVIEWED | Posted: 15 November 2023 doi:10.20944/preprints202311.0972.v1

K_2O	0.44	0.38	0.44	0.53	0.99	1.14	1.48	3.49
TiO_2	1.45	1.41	1.37	1.36	1.96	1.91	2.43	1.93
P_2O_5	0.21	0.21	0.21	0.20	1.15	1.11	0.93	1.05
MnO	0.137	0.146	0.147	0.151	0.164	0.165	0.168	0.151
L.O.I.	1.76	1.77	1.80	1.94	2.02	2.34	2.46	2.57
Total	99.657	99.896	99.437	99.621	99.324	99.525	99.808	100.211
MG	54.26	54.96	55.22	56.05	55.08	56.65	52.67	55.92
				C.I.P.W. Norm				
Q	4.50	2.44	3.68	3.47	-	-	-	-
Qr	2.60	2.25	2.60	3.13	5.85	6.74	8.75	20.63
Ab	23.27	24.29	23.52	24.62	25.79	28.39	27.30	11.03
An	26.06	25.75	25.57	25.01	5.83	5.89	12.45	4.08
Lc	-	-	-	-	-	-	-	-
Ne	-	-	-	-	13.63	11.62	2.72	17.31
Di	11.66	15.15	13.96	11.03	20.29	17.40	24.96	18.36
Hy	24.01	22.58	22.75	24.56	-	-	-	-
Mt	2.54	2.51	2.46	2.45	2.75	2.74	2.64	2.74
Ol	-	-	-	-	16.79	18.21	11.76	17.40
Il	2.75	2.68	2.60	2.58	3.72	3.63	4.62	3.67
Ap	0.50	0.50	0.50	0.47	2.72	2.63	2.20	2.49

Location	Nushan area	Luozhuang area					Banta area	
Sample	AM5	AN1	AN2	AN3	AN4	AN5	AB1	AB2
Rock type	AB	AB	TB	AB	AB	TB	TB	TB
SiO_2(wt%)	46.65	47.56	50.35	44.25	45.15	50.21	51.08	52.33
Al_2O_3	13.79	12.68	13.05	13.53	12.65	13.09	12.96	13.30
ΣFeO	11.16	11.01	10.57	11.40	11.44	10.63	10.89	10.85
MgO	7.90	6.61	5.88	8.22	7.25	5.78	5.35	6.63
CaO	6.44	8.34	8.42	6.34	9.22	8.48	7.44	7.10
Na_2O	5.11	4.24	3.03	5.10	4.55	2.94	3.09	3.31
K_2O	3.28	1.30	1.36	3.57	1.09	1.30	1.46	1.42
TiO_2	1.93	2.43	2.00	1.95	2.05	1.98	1.80	1.75
P_2O_5	1.06	0.98	0.41	1.04	1.06	0.56	0.46	0.43
MnO	0.150	0.156	0.143	0.160	0.125	0.143	0.146	0.158
L.O.I.	2.48	4.48	4.91	4.35	4.80	5.05	5.29	2.37
Total	99.850	99.786	100.123	99.910	99.835	100.163	99.966	99.648
MG	56.03	51.94	50.03	56.48	53.29	49.46	46.93	52.38
			C.I.P.W. Norm					
Q	-	-	1.10	-	-	1.81	2.83	1.33
Qr	19.38	7.68	8.04	21.10	6.44	7.68	8.63	8.39
Ab	14.56	30.97	25.64	7.10	22.39	24.88	26.15	28.01
An	5.00	11.73	17.99	3.48	10.87	18.68	17.18	17.24
Lc	-	-	-	-	-	-	-	-
Ne	15.54	2.66	-	19.53	8.73	-	-	-
Di	16.33	19.02	17.33	17.27	22.82	16.22	13.81	12.44
Hy	-	-	17.82	-	-	18.22	18.97	22.92
Mt	2.70	2.67	2.55	2.75	2.77	2.57	2.64	2.62
Ol	17.74	13.71	-	18.22	13.81	-	-	-
Il	3.67	4.62	3.80	3.70	4.75	3.76	3.42	3.32
Ap	2.51	2.32	0.97	2.46	2.51	1.33	1.09	1.02

Location	Banta area	Niugang area			Shaoji area		Suxiang area
Sample	AB3	AL1	AL2	AL3	AH1	AH2	AS1
Rock type	TB	TB	TB	TB	AB	AB	TB
SiO_2(wt%)	52.26	52.46	53.28	52.45	47.34	46.65	51.09
Al_2O_3	13.24	14.30	13.67	13.99	12.21	12.15	14.03

ΣFeO	10.59	10.07	9.57	9.90	11.97	11.89	10.50
MgO	6.70	3.85	4.26	4.23	6.67	6.53	4.04
CaO	8.25	6.15	7.47	8.06	8.41	8.54	5.40
Na_2O	3.27	3.34	3.44	3.84	4.56	4.15	3.09
K_2O	1.42	2.11	1.97	1.92	1.43	1.13	2.17
TiO_2	1.72	1.91	1.80	1.85	2.65	2.65	2.09
P_2O_5	0.41	0.52	0.49	0.51	0.90	0.98	0.60
MnO	0.155	0.171	0.093	0.117	0.143	0.133	0.089
L.O.I.	1.57	4.58	3.08	3.13	3.97	5.09	6.21
Total	99.585	99.461	99.123	99.637	100.253	99.893	99.309
MG	53.25	40.76	44.48	43.47	50.08	49.71	40.92
			C.I.P.W. Norm				
Q	0.27	4.42	3.80	2.00	-	-	4.79
Qr	8.93	12.47	11.64	11.35	8.45	6.68	12.82
Ab	27.67	28.26	29.11	29.45	27.59	29.93	26.15
An	17.26	17.80	16.04	16.88	8.62	11.19	18.00
Lc	-	-	-	-	-	-	-
Ne	-	-	-	-	5.96	2.81	-
Di	17.20	7.75	14.74	16.38	22.32	20.32	4.05
Hy	20.45	16.91	13.85	13.36	-	-	19.39
Mt	2.57	2.44	2.32	2.39	2.90	2.87	2.54
Ol	-	-	-	-	13.34	13.70	-
Il	3.27	3.63	3.42	3.51	5.03	5.03	3.97
Ap	0.97	1.23	1.16	1.21	2.13	2.32	1.42

[1] AB: Alkali basalt; TB: tholeiite basalt; $M^{\#}$- (Mg-value) = 100*Mg/(Mg + Fe^{+2}).

The graphs illustrating the SiO_2 content in correlation with major and trace element concentrations offer valuable insights into the geological processes occurring during the evolution of basaltic magma. From the plot of SiO_2 content against major elements (Figure 3), it can be observed that MgO, ΣFeO, and Na_2O contents in the study basalts exhibit a weak negative correlation with SiO_2 content. This indicates that during the magma evolution process, these rocks underwent fractional crystallization involving minerals such as olivine, pyroxene, and a small amount of plagioclase. Furthermore, from Figure 3, it appears that the basaltic rocks within the study area can be distinguished into two distinct magma systems: alkali and tholeiite basaltic magmas. Alkali basalts exhibit higher ΣFeO, MgO, Na_2O, TiO_2, and P_2O_5 contents compared to tholeiite basalts.

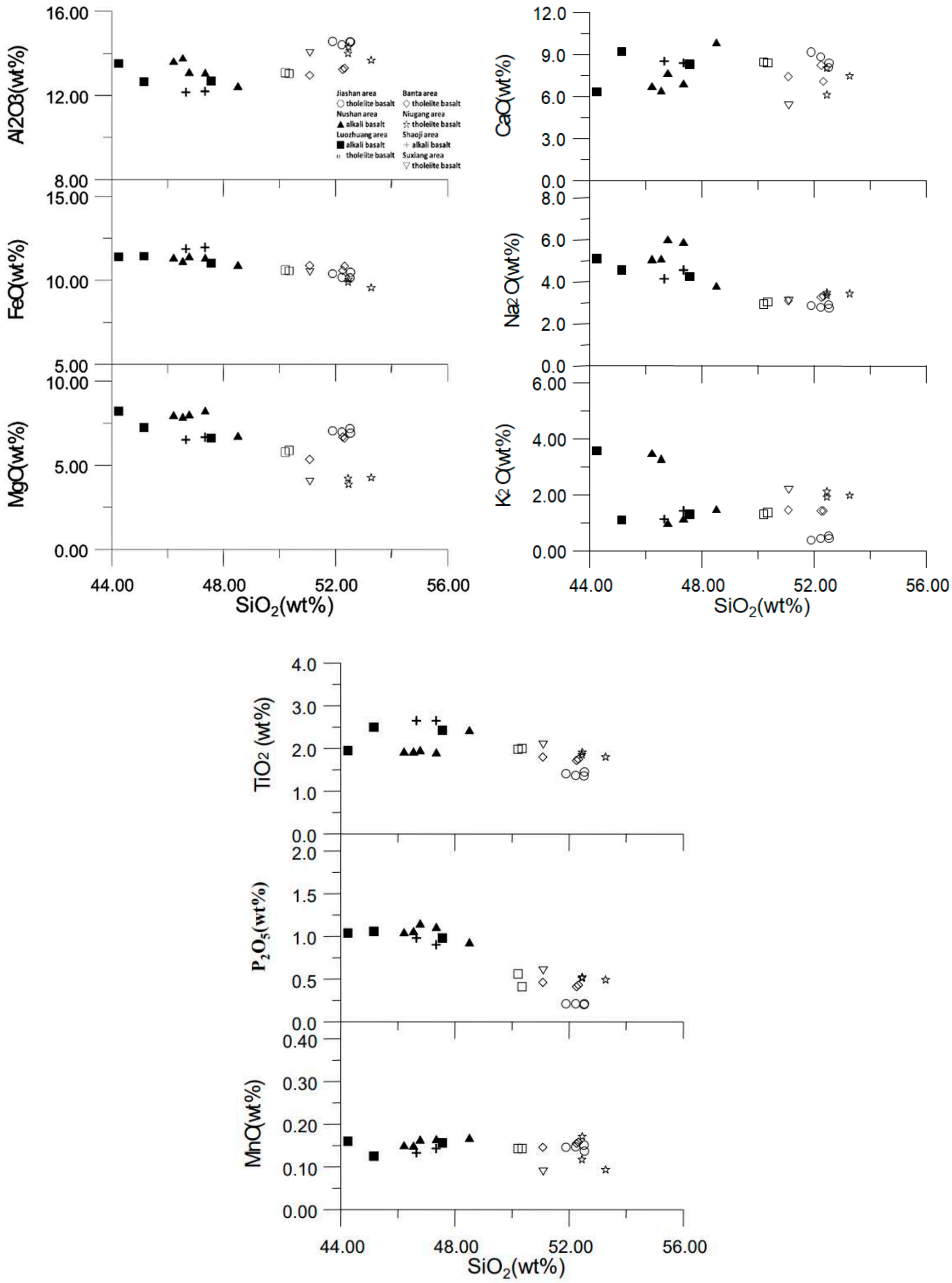

Figure 3. Major elements vs. SiO_2 plots for basaltic rocks from Anhui province.

3.2. Trace element geochemistry

The results of trace element and rare-earth element content analysis of the Cenozoic basalts from the study area are shown in Table 2. Elements such as Ni, Co, Cr, V, Cu, Sc, and Zn, which exhibit significant mineral/melt partition coefficients, serve as sensitive indicators for tracking the fractionation of olivine and clinopyroxene from basaltic magmas. Figure 4 illustrates that the content of compatible elements (Cr, Sc) in the tholeiite basalts of the study is slightly higher than that in alkali basalts. This phenomenon may suggest that alkali basalts are formed from partial melting of the mantle source with a lower degree.

Table 2. Trace and rare earth elements of basaltic rocks from Anhui province.

Location	Jiashan area				Nushan area			
Sample	AG1	AG2	AG3	AG4	AM1	AM2	AM3	AM4
Rock type	TB	TB	TB	TB	AB	AB	AB	AB
Ba(ppm)	318	309	253	242	408	511	548	578
Co	46	45	47	46	48	48	48	46
Cr	210	214	220	217	224	236	260	182
Cs	0.24	0.29	0.21	0.18	1.01	0.96	0.64	1.05
Cu	89	86	77	78	34	36	46	32
Ga	9.0	8.7	9.2	8.9	11.8	12.5	12.2	13.1
Hf	3.4	3.1	2.7	3.0	5.4	5.2	5.6	5.4
Li	10.2	15.0	12.6	9.4	10.2	9.8	13.3	11.5
Nb	8.9	8.6	9.0	8.7	103.1	103.6	74.1	99.5
Ni	151	152	148	151	189	193	191	164
Pb	5.4	2.6	1.2	1.4	3.2	3.9	3.5	3.1
Rb	11.2	10.2	7.9	9.6	52.2	43.3	35.5	51.9
Sc	28.2	24.3	26.8	26.8	13.2	14.2	20.9	14.2
Sr	236	235	251	281	681	681	754	723
Ta	0.70	0.62	0.64	0.54	6.01	5.94	4.31	5.98
Th	1.32	1.04	0.84	0.89	8.37	7.99	5.57	7.77
U	0.37	0.34	0.21	0.24	2.37	2.23	1.49	2.37
V	191	188	203	190	159	151	210	162
Y	24.2	23.0	23.4	23.4	24.3	24.9	27.9	24.1
Zn	95	95	94	93	132	126	107	126
Zr	123	114	121	113	302	297	304	312
La	11.34	10.49	10.20	9.90	61.29	61.87	46.76	55.85
Ce	26.87	25.32	23.56	23.05	106.19	109.54	85.60	99.75
Nd	15.73	14.47	12.53	12.53	48.48	47.21	40.08	43.51
Sm	4.93	4.69	3.75	3.67	9.75	9.96	8.70	8.90
Eu	1.86	1.81	1.32	1.34	3.04	3.01	2.76	2.74
Gd	4.03	3.83	2.59	2.65	5.49	5.46	4.90	5.02
Tb	1.03	0.96	0.69	0.71	1.18	1.15	1.13	1.10
Yb	2.32	2.24	1.72	1.73	1.20	1.16	1.60	1.15
Lu	0.39	0.39	0.22	0.22	0.13	0.13	0.18	0.12

Location	Nushan area	Luozhuang area					Banta area	
Sample	AM5	AN1	AN2	AN3	AN4	AN5	AB1	AB2
Rock type	AB	AB	TB	AB	AB	TB	TB	TB
Ba(ppm)	536	572	499	545	562	469	467	396
Co	45	49	50	45	47	45	57	53
Cr	196	261	269	197	262	272	342	374
Cs	1.02	0.63	0.48	1.05	0.61	0.40	0.14	0.12
Cu	35	50	60	33	52	58	66	65
Ga	13.0	12.8	11.9	12.9	12.5	11.4	11.3	10.5
Hf	5.3	5.8	4.1	5.4	5.9	3.9	3.8	3.5
Li	12.0	8.5	8.4	10.8	14.6	8.0	5.5	5.5
Nb	101.6	81.7	45.4	100.9	88.1	43.3	31.8	28.0
Ni	169	196	216	182	207	197	280	266
Pb	3.2	4.8	4.2	3.0	3.9	2.7	2.6	2.5
Rb	54.9	36.6	21.6	53.9	35.6	19.3	22.2	18.5
Sc	13.0	22.5	24.1	13.9	19.5	21.7	22.5	22.0
Sr	579	698	466	675	797	389	382	329
Ta	5.70	4.66	2.70	5.90	5.00	2.42	1.86	1.59
Th	7.16	6.57	3.18	7.22	6.91	2.78	2.59	2.12
U	2.08	1.59	0.57	2.25	1.7	0.49	0.51	0.51
V	163	247	228	168	226	224	225	207
Y	23.6	31.0	24.8	24.4	30.5	23.8	25.9	22.6
Zn	126	109	105	132	120	112	115	104

Zr	312	337	216	316	350	207	183	180
La	54.63	50.76	29.21	56.27	54.20	27.30	22.69	19.92
Ce	97.62	93.07	56.90	100.28	99.21	53.21	46.04	40.78
Nd	42.01	42.74	26.51	43.54	46.29	25.20	22.21	19.32
Sm	8.63	9.23	6.20	8.73	9.76	5.89	5.76	4.98
Eu	2.72	2.95	2.08	2.78	3.09	1.99	1.91	1.66
Gd	4.71	5.16	3.84	5.12	5.39	3.55	3.54	3.16
Tb	1.06	1.23	0.95	1.07	1.26	0.90	0.90	0.79
Yb	1.13	1.63	1.57	1.09	1.56	1.45	1.68	1.45
Lu	0.13	0.22	0.21	0.12	0.19	0.20	0.30	0.18

Location	**Banta area**	**Niugang area**			**Shaoji area**		**Suxiang area**
Sample	AB3	AL1	AL2	AL3	AH1	AH2	AS1
Rock type	TB	TB	TB	TB	AB	AB	TB
Ba(ppm)	371	996	778	845	538	493	914
Co	49	42	32	38	42	46	38
Cr	329	237	211	202	154	153	279
Cs	0.15	0.25	0.21	0.24	0.78	0.65	0.15
Cu	64	62	66	68	44	45	61
Ga	10.6	16.4	14.2	14.8	12.6	14.0	15.6
Hf	3.9	3.9	3.8	4.0	6.0	6.6	4.9
Li	5.4	8.6	7.1	7.6	8.5	9.7	9.4
Nb	27.7	38.7	34.6	35.6	84.1	91.6	41.0
Ni	220	97	92	94	128	128	121
Pb	2.8	6.6	4.7	5.2	3.1	3.7	6.2
Rb	19.1	35.5	31.4	32.5	43.5	66.2	33.6
Sc	23.4	20.9	20.4	20.4	15.3	14.9	19.4
Sr	375	282	397	346	795	717	316
Ta	1.64	2.20	1.83	1.97	5.26	4.82	1.97
Th	2.42	3.87	3.29	3.45	6.50	5.95	4.15
U	0.72	0.75	0.63	0.70	1.77	1.80	1.06
V	197	187	175	178	226	252	174
Y	23.2	27.1	25.7	26.10	26.7	26.20	26.0
Zn	102	100	198	100	144	129	102
Zr	180	177	202	201	322	267	179
La	19.99	46.37	38.79	40.53	49.76	47.13	43.49
Ce	41.10	88.78	73.27	79.57	92.54	93.64	72.96
Nd	20.45	39.91	32.88	35.01	43.30	44.15	39.38
Sm	5.15	8.30	7.06	7.31	9.30	10.03	8.32
Eu	1.76	2.55	2.17	2.30	3.02	2.94	2.64
Gd	3.35	4.80	4.16	4.33	5.05	8.69	7.18
Tb	0.82	1.08	0.95	0.97	1.20	1.20	1.07
Yb	1.61	1.76	1.47	1.53	1.28	1.25	1.78
Lu	0.26	0.23	0.21	0.20	0.20	0.15	0.22

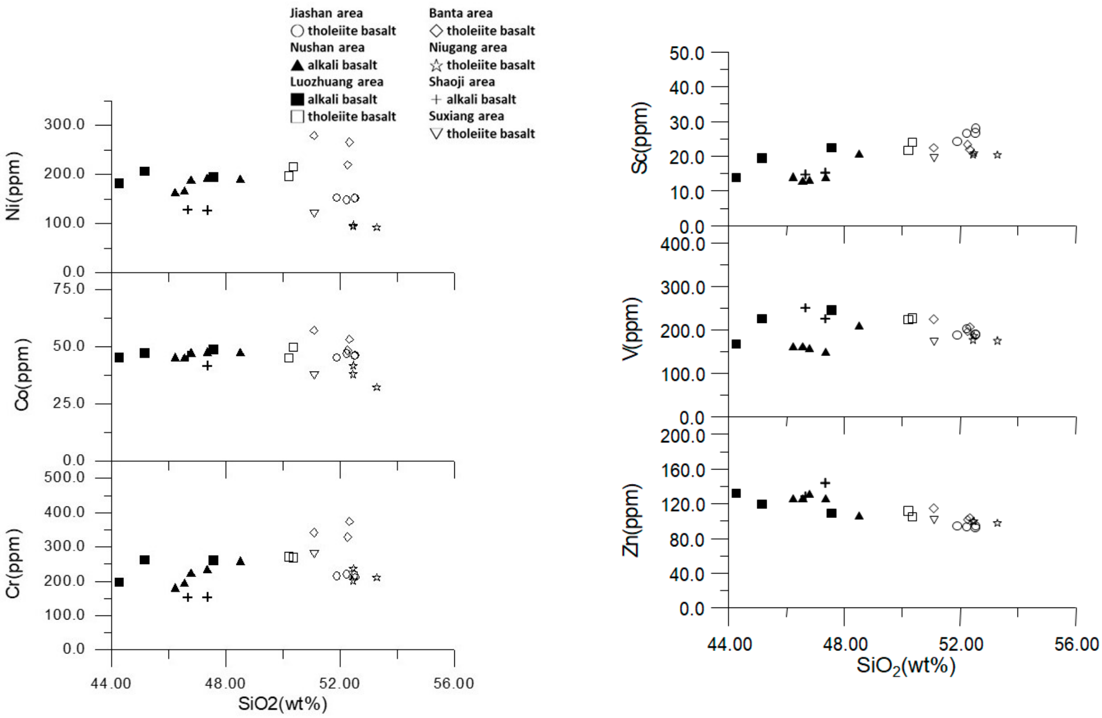

Figure 4. Compatible elements vs. SiO_2 plots for basaltic rocks from Anhui province.

It is widely recognized that elements with high incompatibility do not segregate from one another during processes like partial melting or fractional crystallization. Instead, their ratios in the resulting materials reflect those of the source regions [15]. The plot of incompatible elements against SiO_2 content for the basalts in this study is shown in Figure 5. The figure clearly shows that alkali basalts exhibit significantly higher contents of incompatible elements compared to tholeiite basalts. This phenomenon is likely a result of these two magma systems originating from different degrees of partial melting of the mantle source. Furthermore, the figure indicates that in the tholeiite basalts of Niugang and Suxiang areas, the content of Ba, Pb, and Rb is higher compared to other tholeiite basalts. We suggest that this may be due to the presence of higher potassium-bearing minerals in these basalts or possibly the result of crustal contamination. Based on observations of rock thin sections, we have determined that the tholeiite basalts of Niugang and Suxiang areas contain higher amounts of leucite. Therefore, it is concluded that this may be due to the presence of leucite in these basalts.

 doi:10.20944/preprints202311.0972.v1

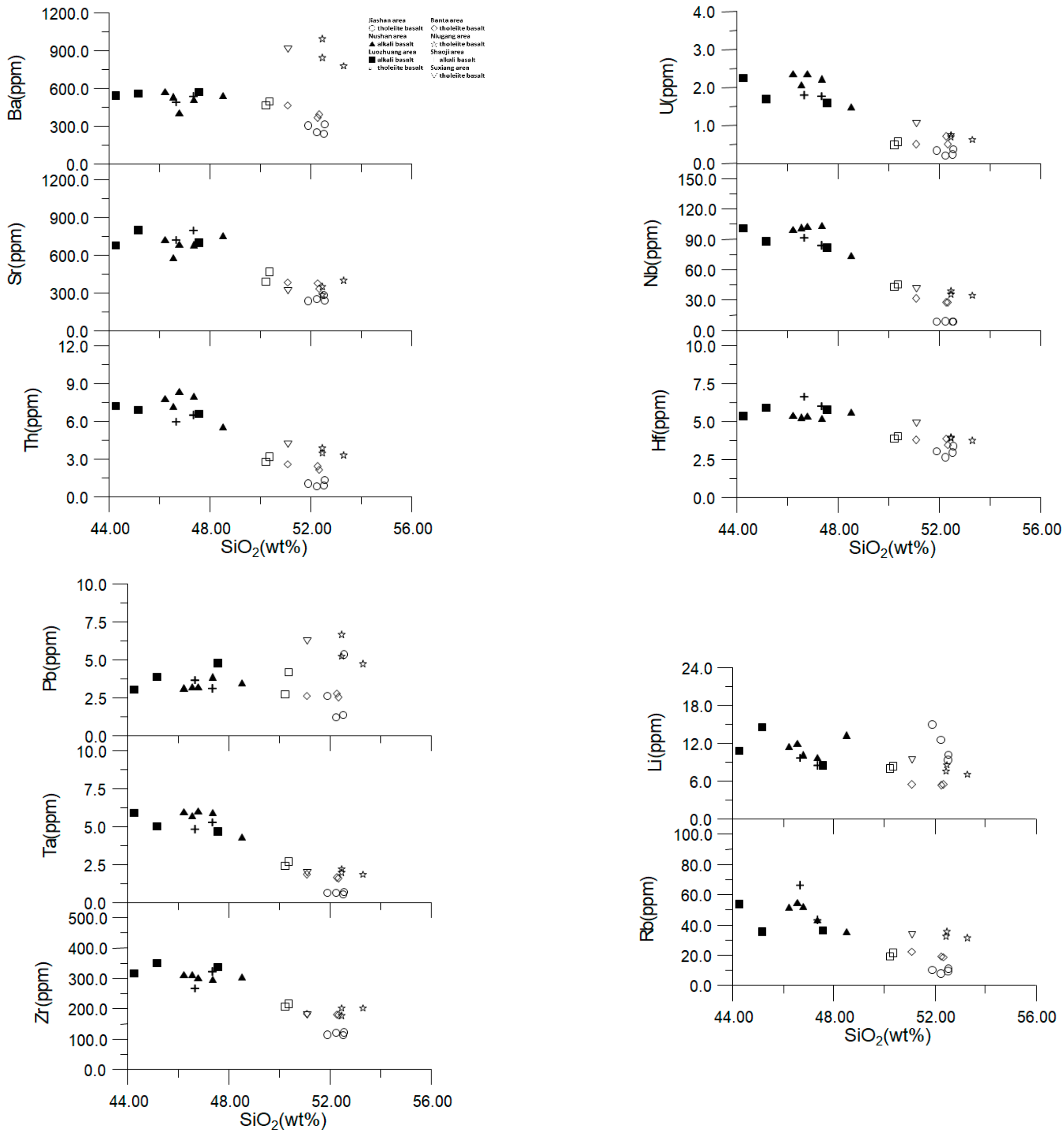

Figure 5. Incompatible elements vs. SiO_2 plots for basaltic rocks from Anhui province.

The diagrams in Figure 6 display primitive mantle-normalized incompatible element patterns for basaltic rocks from Anhui province. Most of the basaltic samples in this study exhibit elevated levels of large ion lithophile elements (LILE) and light rare earth elements (REE), similar to those found in the average oceanic island basalt as suggested by Sun and McDonough (1989) [16]. Moreover, these samples do not exhibit significant depletions in niobium (Nb), suggesting that the possibility of crustal contamination during magma generation may be not significant. Most alkali basalts of the study exhibit negative anomalies in K and Sr, while tholeiite basalts show a positive anomaly in Ba. Overall, most types of basalts in the present study display positive anomalies in Nb and slight positive anomalies in Ti.

Preprints (www.preprints.org) | NOT PEER-REVIEWED | Posted: 15 November 2023 doi:10.20944/preprints202311.0972.v1

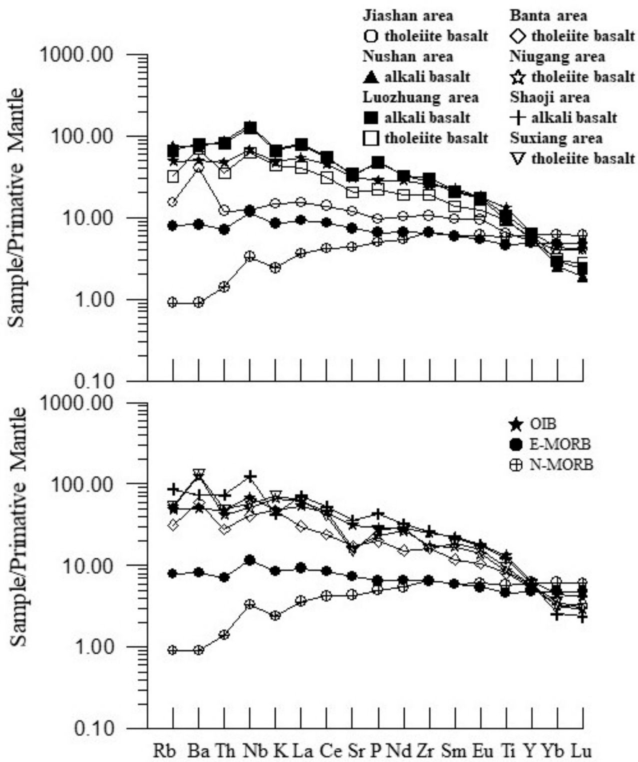

Figure 6. Primitive mantle normalized incompatible element patterns for average basaltic rocks from Anhui province. OIB, N-MORB, E-MORB and primitive mantle data are from Sun and McDonough (1989) [16].

The rare-earth elements (REEs) hold significant importance as trace elements in the investigation of parent rock petrogenesis, as their patterns remain unaffected by melting or metamorphic processes. The Rare Earth Element (REE) distribution in an igneous rock is influenced by the REE chemistry of its source. Figure 7 illustrates the chondrite-normalized rare earth element (REE) patterns of the basaltic rocks analyzed in this study, in comparison with the patterns observed in Ocean Island Basalts (OIB), Enriched Mid-Ocean Ridge Basalts (E-MORB), and Normal Mid-Ocean Ridge Basalts (N-MORB). The patterns resemble those of OIB, indicating an enrichment in LREE and a mantle composition similar to OIB. In general, the alkali basalts in the study area exhibit higher rare earth element (REE) content compared to the tholeiite basalts. However, the light rare earth elements (La, Ce, and Nd) and middle rare earth elements (Sm, Eu, and Gd) in the tholeiite basalts of Niugang and Suxiang areas are higher than those in tholeiite basalts from other areas. Xu and Bodinier (2004) [14] revealed that amphibole-bearing peridotites from Nushan region contain higher concentrations of light rare earth elements and middle rare earth elements compared to amphibole-free peridotites, while the heavy rare earth elements in both groups show similar levels. We suggest that the mantle source region of the basalt in Niugang and Suxiang areas may contain a significant amount of amphibole-bearing peridotites. Consequently, during partial melting processes, the basalt in this area exhibits higher concentrations of light rare earth elements and middle rare earth elements.

Preprints (www.preprints.org) | NOT PEER-REVIEWED | Posted: 15 November 2023 doi:10.20944/preprints202311.0972.v1

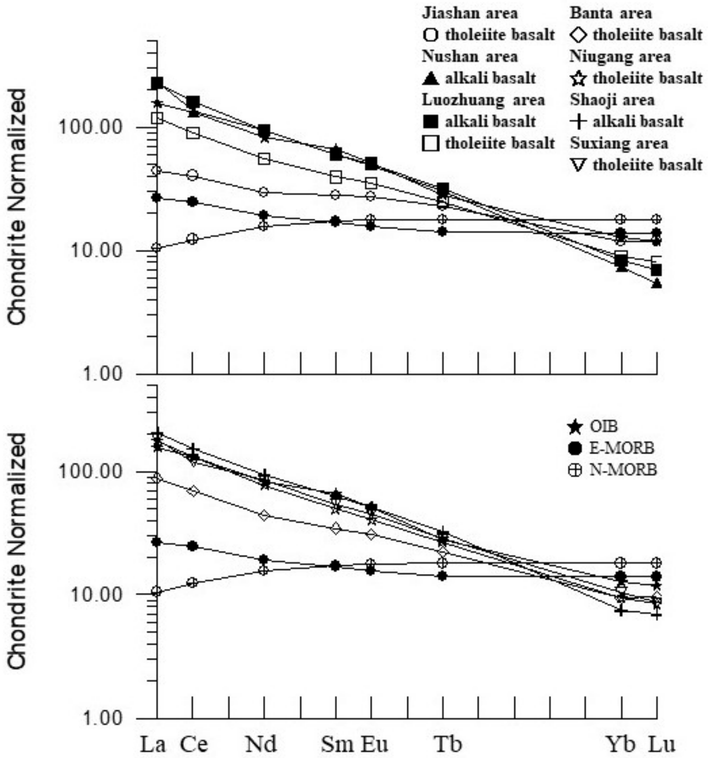

Figure 7. Average REE composition of basaltic rocks from Anhui province as compared with OIB, N-MORB and E-MORB (Sun and McDonough,1989) [16].

3.3. Isotope geochemistry

Zou et al. (2000) [17] concluded that basalts across eastern China consistently exhibit high $^{208}Pb/^{204}Pb$ and $^{207}Pb/^{204}Pb$ ratios for a given $^{206}Pb/^{204}Pb$ ratio, a characteristic commonly observed in Dupal oceanic island basalts in the Southern Hemisphere. Furthermore, the isotopic data from basalts in Southeast China provide support for Li's (1994) [18] crustal detachment model, indicating that a subsurface suture between the South China and North China Blocks extends eastward through Nanjing. The basalts in the Nushan region exhibit the highest $^{143}Nd/^{144}Nd$ and the lowest $^{87}Sr/^{86}Sr$ ratios, possibly representing the isotopic composition of the asthenospheric mantle. Based on Hf-Nd isotope data from Mesozoic-Cenozoic basaltic lavas in the Liaoning, Shandong, Hebei, and Jiangsu-Anhui regions within the North China Craton (NCC), Meng et al. (2015) [19] proposed that lavas older than 110 Ma probably originated primarily from the "ancient metasomatized lithosphere" or may contain contributions from ancient continental crust during lithospheric thinning. On the other hand, lavas younger than 110 Ma, characterized by more depleted Sr-Nd-Hf isotopic compositions, are likely to have originated from the asthenosphere after the lithosphere had already undergone thinning, with the ancient lithospheric mantle having been removed. The Sr-Nd isotope compositions of Cenozoic basalts from Anhui Province are presented in Table 3. Basaltic rocks from Anhui province exhibit a diverse isotopic composition, with $^{87}Sr/^{86}Sr$ ratios ranging from 0.703215 to 0.706053 and $^{143}Nd/^{144}Nd$ ratios ranging from 0.511967 to 0.512981. These variations suggest a heterogeneous mantle source for these rocks. The plot of $^{87}Sr/^{86}Sr$ versus $^{143}Nd/^{144}Nd$ (Figure 8) reveals that the basaltic rocks in Anhui Province fall between MORB and EM-I components. This suggests that the basaltic rocks in the study area possibly originate from a mantle source with characteristics representing both MORB and EM-I end-members.

Table 3. The Sr-Nd isotope compositions of Cenozoic basalts from Anhui Province.

Sample No.	Location	Rock type	$^{87}Sr/^{86}Sr$	$^{143}Nd/^{144}Nd$
[1]AJSN-1	Nushan	Alkali basalt	0.70345	0.512964
[1]AJSN-2	Jiashan	Tholeiite basalt	0.70437	0.512615
[1]AHFD-2	Dashushan	Alkali basalt	0.70465	0.512803
[1]ADTF-4	Dangtu	Alkali basalt	0.70466	0.512748
[2]AB3	Banta	Tholeiite basalt	0.704523	0.512556
[2]AG4	Jiashan	Tholeiite basalt	0.706053	0.512340
[2]AL2	Niugang	Tholeiite basalt	0.705484	0.511967
[2]AM2	Nushan	Alkali basalt	0.703290	0.512957
[2]AN2	Luozhuang	Tholeiite basalt	0.704188	0.512679
[3]NS-1	Nushan	Alkali basalt	0.703215	0.512981

[1] Chen et al. (1990) [20]; [2]This study;[3]Zou et al. (2000) [17].

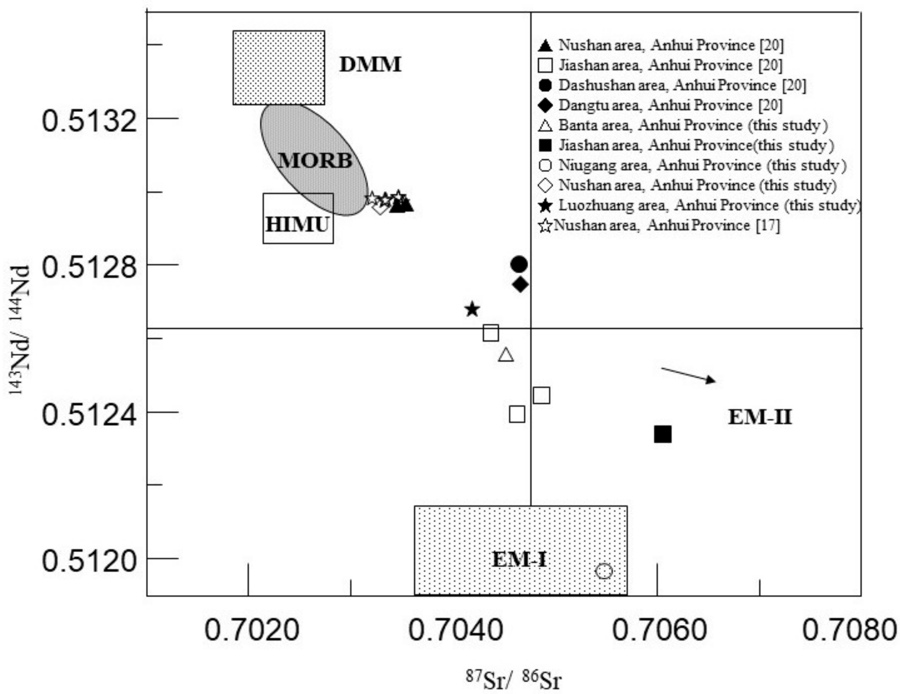

Figure 8. $^{143}Nd/^{144}Nd$ vs. $^{87}Sr/^{86}Sr$ plots for basaltic rocks from Anhui province.

The ^{40}Ar-^{39}Ar dating results for five selected samples from Anhui province are presented in Table 4. The ^{40}Ar-^{39}Ar ages of five basaltic rocks range from 0.56±0.25 to 31.1±0.5 Ma. Combining the ^{40}Ar-^{39}Ar dating results obtained in this study with the K-Ar dating results from Chen and Peng (1988) [21] (Table 4), volcanic eruptions within Anhui Province can be categorized into four periods: early Tertiary (Datong Fushan: 53.18 Ma), Oligocene (Jiashan area, Hefei Dashushan, Jiashan Dahengshan: 31.1-37.58 Ma), Miocene (Jiashan Qingmingshan, Niugang area, Banta area, Suxiang area: 6.9-18.59 Ma), and Pleistocene (Nushan: 0.53-0.73 Ma).

Table 4. The K-Ar and Ar-Ar dating results for the basaltic rocks from Anhui Province.

Sample No.	Location	Rock type	Ma
[1]AJS-3	Jiashan Mingguang	Tholeiite basalt	65.02
[1]AJS-5	Jiashan Mingguang	Tholeiite basalt	54.79
[1]ADTF-4	Dangtu	Alkali basalt	53.18
[1]AHFD-2	Dashushan	Alkali basalt	36.19

[1]AJSD-1	Jiashan Dahengshan	Tholeiite basalt	37.58
[1]AJSQ-1	Jiashan Qingmingshan	Olivine Tholeiite	16.52
[1]AJSQ-2	Jiashan Qing-mingshan	Olivine Tholeiite	15.41
[1]AJSN-1	Nushan	Alkali basalt	0.726
[1]AJSN-2	Nushan	Alkali basalt	0.530
[1]AJSN-3	Nushan	Alkali basalt	0.567
			^{40}Ar-^{39}Ar
[2]AG4	Jiashan	Tholeiite basalt	31.1±0.5
[2]AB3	Banta	Tholeiite basalt	18.59±0.18
[2]AL2	Niugang	Tholeiite basalt	14.42±0.48
[2]AS1	Luozhuang	Tholeiite basalt	6.90±0.15
[2]AM2	Nushan	Alkali basalt	0.56±0.25

[1] Chen and Peng (1988) [21]; [2]This study.

4. Discussion

4.1. Geochemical characteristics of Anihui basalts and implications for their mantle sources

Basaltic magma is generated through partial melting of upper mantle materials such as garnet lherzolites and spinel lherzolites. If such magma had not undergone significant fractional crystallization or contamination by crustal materials since their formation, it can be regarded as a primary magma. The chemical composition of this magma is primarily influenced by the mineral composition, chemical characteristics of the mantle source region, as well as the temperature, pressure conditions during its formation, and the degree of partial melting. Such magmas typically exhibit high contents of Ni and Cr and have high magnesium values.

Previous research findings indicate that the origins of basalts in northeastern China have been explained as a result of mixing between a mantle with depleted isotopes and an EM1 mantle [22–28]. In contrast, the sources of basalts in southeastern China have been identified as a mixture of a depleted mantle and an EM2 mantle [17,29]. The enriched elements found in Cenozoic basalts in eastern China are widely believed to be closely linked to the subducted Pacific slab [30–32]. Specifically, the EM1 components observed in intracontinental basalts erupted in eastern China are thought to be associated with the dehydration process occurring in the subducted Pacific slab.

Based on the chemical compositions of basalts from western Shandong and Bohai Bay Basin, Li et al. (2016) [33] proposed that the asthenospheric mantle beneath the eastern North China Craton (NCC) - containing garnet pyroxenite with an EM1 isotopic signature - underwent metasomatism due to carbonatitic melts. These melts were derived from carbonated eclogite, originating from subducted Pacific slab materials present in the deeper mantle.

The content of incompatible elements in basalt is primarily controlled by the degree of partial melting in the mantle source and is less likely to change due to fractional crystallization processes. Therefore, the ratios of incompatible elements in basalt are often used to investigate the chemical characteristics of the magma source region. Furthermore, the isotope ratios (Sr, Nd, and Pb isotopes) in basalt, unaffected by factors such as partial melting and fractional crystallization processes during magma evolution, often reflect the characteristic isotope composition of the mantle source region. The incompatible elements and rare earth element contents in various types of basalts of the study area are similar to oceanic island basalts (Figures 6 and 7), displaying characteristics of enrichment in incompatible elements and rare earth elements. Based on previous studies [34,35], it has been suggested that the mantle source region in the Nushan area contains phlogopite peridotites at depths of 30 to 40 kilometers. We suggest that the negative anomalies in K and Sr observed in the alkali basalts of the study may be related to the abundance of phlogopite in the spinel lherzolite of the mantle source region, and it appears that phlogopite has not involved in the partial melting process. Xu and Bodinier (2004) [14] propose that the mantle source in Nushan region may have undergone

 doi:10.20944/preprints202311.0972.v1

metasomatic processes following the thinning of the lithosphere during the Late Mesozoic. Most of the basaltic rocks exhibit positive anomalies in Nb and slight positive anomalies in Ti which indicate that titanium-bearing minerals of the mantle source region may have been involved in partial melting and the mantle source region may have undergone metasomatic processes.

All types of basalts in the study area exhibit a depletion in heavy rare earth elements (Yb and Lu). The heavy rare earth elements are hosted in garnet, with distribution coefficients for Yb and Lu estimated at 35.6 and 41, respectively [36]. The depletion of heavy rare earth elements (Yb and Lu) observed in the studied basaltic rocks could be explained by the existence of garnet peridotite in the upper mantle, where garnet can hold back heavy rare earth elements (Yb and Lu). Xu et al. (1998) [37], in their study of the Cenozoic lithosphere in the Nushan area of Anhui Province, suggested that the thickness of the lithosphere in this region is approximately 100 kilometers. They found garnet lherzolite at depths ranging from 65 to 100 kilometers. Additionally, spinel peridotites containing amphibole were found in the region, indicating the mantle source in this area may have undergone metasomatic processes.

In the Zr-Y diagram (Figure 9), the ratios of basalts within the study area show a wide range of variation, but most data points are close to Oceanic Island Basalts (OIB), indicating an enriched mantle source. The tholeiite basalts in the Jiashan area are closer to E-MORB, possibly due to higher degree of partial melting (approximately 15%) or originating from a mantle source relatively unaffected by metasomatism. However, based on the Sr-Nd isotopic data (Figure 8), it is apparent that the mantle source in this area is more closely related to an EMI-type enriched mantle. Therefore, we suggest that the source of tholeiite basalts in the Jiashan area may be amphibole-free lherzolite, and these lherzolite might have undergone wall-rock metasomatism [14]. Subsequently, a higher degree of partial melting resulted in lower contents of incompatible elements and rare earth elements in the tholeiite basalts of this area. Additionally, the data points for the basalts in the Nushan area are predominantly close to MORB, indicating that the mantle source in the Nushan area might be a depleted asthenospheric mantle. The basalt in Niugang area falls within the enrichment mantle source type EM-I. These basalts likely represent the mantle end components of the EM-I enriched mantle source in this area. Therefore, we propose that the Anhui basalts may have originated from the partial melting of a mantle source representing a mixing of two end-members: DMM (Depleted MORB Mantle) and EM-I (Enriched Mantle 1). Some of the Anhui basaltic magmas may have originated from the partial melting of EM-I, potentially influenced by upwelling asthenospheric mantle or asthenospheric diapirism processes.

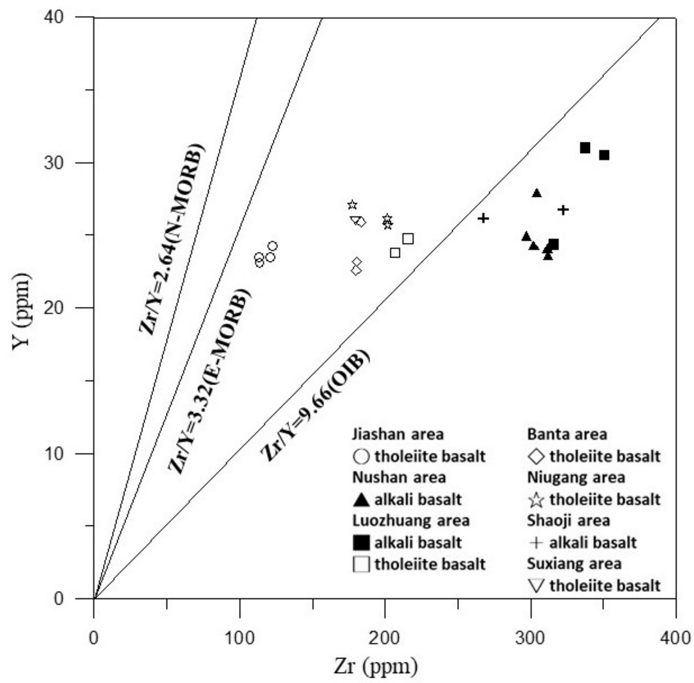

Preprints (www.preprints.org) | NOT PEER-REVIEWED | Posted: 15 November 2023 doi:10.20944/preprints202311.0972.v1

Figure 9. The Y vs. Zr plots for basaltic rocks from Anhui province. OIB, N-MORB and E-MORB data are from Sun and McDonough (1989) [16].

Xu et al. (2017) [38] point out the Cenozoic continental basalts in east-central China exhibit trace element patterns resembling those of Ocean Island Basalts (OIB), but with Sr-Nd isotope compositions ranging from more depleted to less enriched values. These distinctive geochemical features are believed to result from diverse contributions to their mantle sources originating from crustal components in the oceanic subduction zone. The westward subduction of the Pacific slab beneath the North China Craton is thought to result in two significant effects. Firstly, it may replace the ancient refractory lithospheric mantle with the depleted MORB mantle. Secondly, this process incorporates crustal components into the mantle sources of continental basalts. Li et al. (2016) [33] propose that the asthenospheric mantle beneath the eastern North China Craton (NCC), containing garnet pyroxenite with an EM1 isotopic signature, underwent metasomatism due to carbonatitic melts originating from carbonated eclogite derived from subducted Pacific slab materials that exist in the deeper mantle. Based on the study of the $\delta^{44/42}Ca$ isotopic ratios observed in 21 selected Cenozoic basaltic lavas from eastern China, Wang et al. (2023) [39] have suggested that carbonatitic metasomatism may play a significant role in the sources beneath eastern China. Figure 10 illustrates the Zr/Sm vs. Hf/Sm diagram for the Cenozoic basalts in the Shandong, Anhui, and Jiangsu provinces. The diagram suggests that the source regions of the basaltic magmas may have undergone varying degrees of carbonate metasomatism before magma generation [40–43]. The correlation observed in the plot of La/Nb versus $^{87}Sr/^{86}Sr$ ratios of basaltic rocks from Shandong, Anhui, and Jiangsu provinces (Fig. 11) implies a positive relationship. This finding suggests that the enrichment of the lithospheric mantle beneath the current study area could be linked to an ancient subduction process. However, it's important to note that the possibility of crustal assimilation cannot be entirely ruled out. Combining the geochemical characteristics in the studied basalts with previous research [38–43], we propose that the underlying mantle source in Anhui province may have undergone metasomatism due to the carbonatitic melts. These melts are believed to have originated from carbonated eclogite, derived from subducted Pacific slab materials present in the deeper mantle.

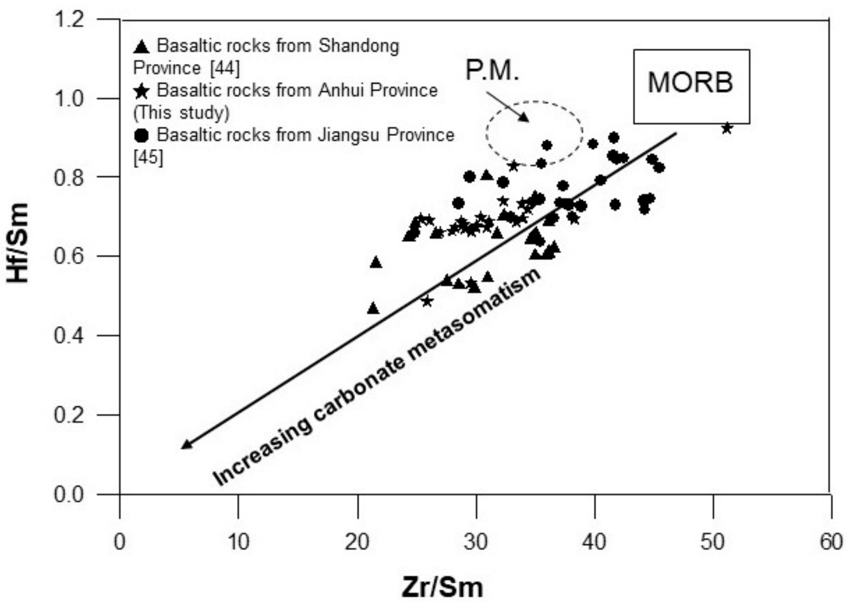

Figure 10. The Zr/Sm vs. Hf/Sm plots for basaltic rocks from Shandong, Anhui and Jiangsu province. Primitive Mantle and MORB data are from Sun and McDonough (1989) [16].

Preprints (www.preprints.org) | NOT PEER-REVIEWED | Posted: 15 November 2023 doi:10.20944/preprints202311.0972.v1

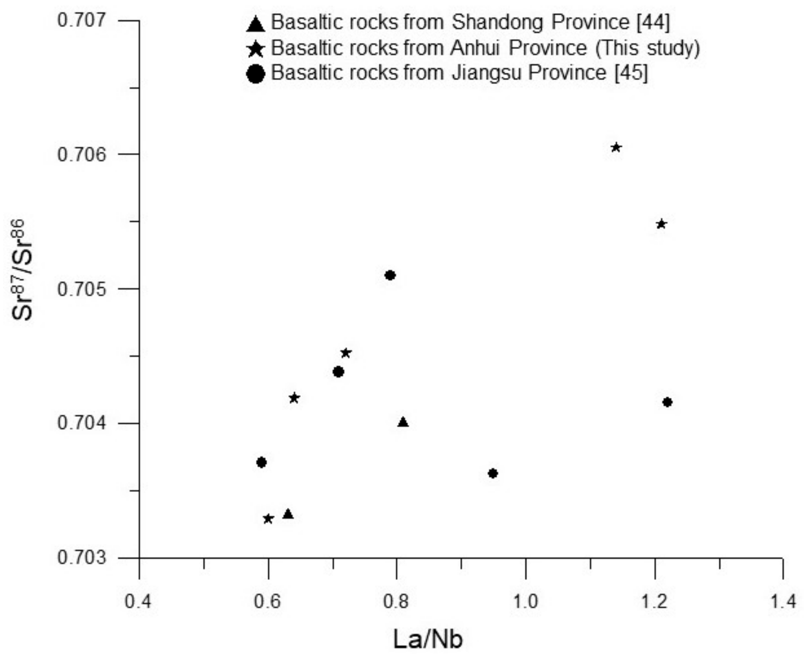

Figure 11. The La/Nb vs. $^{87}Sr/^{86}Sr$ plots for basaltic rocks from Shandong, Anhui and Jiangsu province.

4.2. Petrogenesis of the Basaltic Rocks from Anihui province

Based on the major, trace element, and isotope data of the Cenozoic basalts in the study area, it is indicated that the basalts in this region can be classified into three distinct magma systems: alkali basalts, tholeiite basalts, and Nushan alkali basalts. Zou et al. (2000) [4] suggested that the Cenozoic basaltic rocks in the Nushan area originated through partial melting of a mantle source enriched in light rare earth elements (LREE), with a degree of partial melting ranging from 4% to 11%. Primary magma is the partial melting of basaltic magma from the mantle source region, which has not undergone significant fractional crystallization and crustal contamination. Generally, this magma has higher Ni, Cr content, and magnesium values [46–48]. In this study, samples numbers AM2, AG4, and AN4 are regarded as the parent magmas of Nushan alkali basalt, tholeiite basalt, and alkali basalt, respectively. Based on the calculation using Shaw's equation (1970) [49], we calculated that that partial melting of 1-5%, 15%, and 1-10% of the source mantle can respectively form alkali basalt, tholeiite basalt, and Nushan alkali basalt parent magmas in the study area.

According to Ar-Ar ages of this study and fractional crystallization model established by Brook and Nielsen (1982) [50] as shown in Figure 12, the basalt from Jiashan area (AG4 = 31.1 Ma) may represents the primary magma of the tholeiite basaltic magma system. Subsequently, it gradually underwent fractional crystallization to sequentially form the tholeiite basalts at Banta area (AB3 = 18.59 Ma), Niugang area (AL2 = 14.42 Ma), and Suxiang area (AS1 = 6.9 Ma). The alkali basalt in Luozhuang area (sample number AN4), formed through 1% to 5% partial melting of the mantle source and underwent fractional crystallization primarily involving olivine and clinopyroxene, resulting in the alkali basalt in the region. The alkali basalts in the Nushan area (sample number AM2) were formed through partial melting of the mantle source, estimated to be between 1% and 10%. This parental magma then underwent fractional crystallization primarily involving olivine, clinopyroxene, and plagioclase to produce the basalts in the Nushan area. The chemical differences observed between alkali basalts and tholeiite basalts in this study area may be attributed to varying degrees of partial melting from the mantle source.

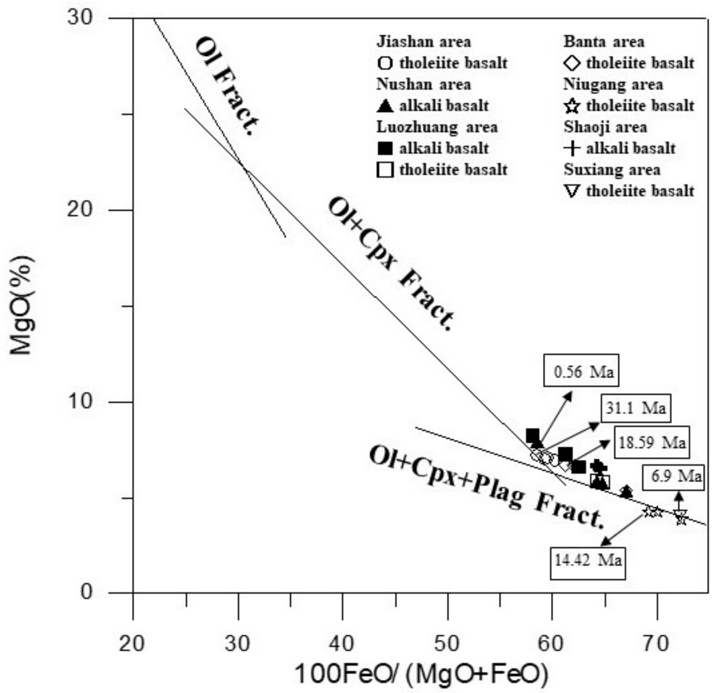

Figure 12. The MgO vs. 100*FeO/(MgO+FeO) plots for basaltic rocks from Anhui province. Fractionation model modified from Brooks and Nielsen (1982) [50]. Numbers are ^{40}Ar-^{39}Ar dating results (in Ma).

5. Conclusions

Based on the major and trace element data, our findings suggest that the basaltic magma underwent a process of fractional crystallization involving olivine, clinopyroxene, and minor plagioclase during its evolution. The chemical compositions of the basaltic rocks in Anhui province indicate the presence of several distinct magmatic series within the study area. Combining the ^{40}Ar-^{39}Ar dating results obtained in this study with the K-Ar dating results from Chen and Peng (1988) [21], basaltic rocks volcanic eruptions within Anhui Province can be categorized into four periods: early Tertiary, Oligocene, Miocene, and Pleistocene. The incompatible elements and rare earth element contents in various types of basalts of the study area are similar to oceanic island basalts, displaying characteristics of enrichment in incompatible elements and rare earth elements. Most of the basaltic rocks exhibit positive anomalies in Nb and slight positive anomalies in Ti which indicate that titanium-bearing minerals of the mantle source region may have been involved in partial melting and the mantle source region may have undergone metasomatic processes. We suggest that the enrichment of the lithospheric mantle beneath the current study area could be linked to an ancient subduction process. Through Sr vs. Nd isotopic ratio plots, we propose that the Anhui basalts may have originated from the partial melting of a mantle source representing a mixing of two end-members: DMM (Depleted MORB Mantle) and EM-I (Enriched Mantle 1). Some of the Anhui basaltic magmas may have originated from the partial melting of EM-I, potentially influenced by upwelling asthenospheric mantle or asthenospheric diapirism processes. The source mantle in the study area undergoes partial melting of 1-5%, 15%, and 1-10%, forming alkaline basalt, tholeiite basalt, and Nushan alkali basalt parent magmas. Subsequently, these parent magmas underwent fractional crystallization processes to produce various types of basalt in the study area.

Author Contributions: Conceptualization, Y.T. Lee; methodology, Y.T. Lee; writing—original draft preparation, Y.T. Lee and M. L. Lin; writing—review and editing, Y.T. Lee and M. L. Lin. All authors have read and agreed to the published version of the manuscript.

Funding: This study is supported by the National Science Council located in Taipei.

 doi:10.20944/preprints202311.0972.v1

Data Availability Statement: All data are presented in this paper.

Acknowledgments: We would like to thank Dr. C. H. Lo of Department of Geosciences of National Taiwan University for his kind assistance in Ar-Ar dating.

Conflicts of Interest: The authors declare no conflict of interest.

References

1. Huang, X. L.; Xu, Y. G.; Liu, D. Y. Geochronology, petrology and geochemistry of the granulite xenolith from Nushan, east China: Implication for a heterogeneous lower crust beneath the Sino-Korean Craton. *Geochim. Cosmochim. Acta.* **2004**, *68*, 127–149.
2. Jahn B. M.; Auvray B.; Cornichet J.; Bai Y. L.; Shen Q. H.; Liu D. Y. 3.5 Ga old amphibolites from eastern Hebei province, China: field occurrence, petrography, Sm-Nd isochron age and REE geochemistry. *Precambrian Res.* **1987**, *34*, 311–346.
3. Liu, R. X.; Chen, W. J.; Sun, J. Z.; Li, D. M. The K-Ar age and tectonic environment of Cenozoic volcanic rocks in China. In Liu, R. X., ed. The age and geochemistry of Cenozoic volcanic rocks in China. *The Seismic Press, Beijing*, 1992,1-43. (In Chinese).
4. Zou, H.; Zindler, A.; Xu, X.; Qi, Q. Major, trace element, and Nd, Sr and Pb isotope studies of Cenozoic basalts in SE China: mantle sources, regional variations, and tectonic significance. *Chem. Geol.* **2000**, *171*, 33-47.
5. Xu, Y. G. Thermo-tectonic destruction of the Archaean lithospheric keel beneath eastern China: evidence, timing and mechanism. *Phys. Chem. Earth* **2001**, *26*, 747-757.
6. Gao, S.; Rudnick, R. L.; Carlson, R. W.; McDonough, W. F.; Liu, Y. S. Re-Os evidence for replacement of ancient mantle lithosphere beneath the North China craton. *Earth Planet. Sci. Lett.* **2002**, *198*, 307-322.
7. Xu Y. G.; Chung S. L.; Ma J.; Shi L. Contrasting Cenozoic lithospheric evolution and architecture in the western and eastern Sino-Korean craton: constraints from geochemistry of basalts and mantle xenoliths. *J. Geol.* **2004**, *112*, 593-605.
8. Zhang, H.H.; Xu, Y.G.; Ge,W.C.; Ma, J.L. 2006, Geochemistry of late Mesozoic–Cenozoic basalts in Yitong–Datun area. Jilin Province and its implication. *Acta Petrol. Sin.* **2006**, *22*, 1579–1607.
9. Sun, J.; Zhu, X.K.; Belshaw, N.S.; Chen, W.; Doroshkevich, A.G.; Luo, W.J.; Song, W.L.; Chen, B.B.; Cheng, Z.G.; Li, Z.H., Wang, Y.; Kynicky, J.; Henderson, G.M. Ca isotope systematics of carbonatites: insights into carbonatite source and evolution. *Geochem. Perspect. Lett.* **2021**, 11–15.
10. Smith, A. D.; Huang, L. Y. The use of extraction chromatographic materials in procedures for the isotopic analysis of neodymium and strontium in rocks by thermal ionisation mass spectrometry. *J. National Cheng-Kung University* **1997**, *32*, 1–10.
11. Odin, G. S.; 35 collaborators. Interlaboratory standards for dating potassium –argon age determinations. In: Odin, G. S. (Ed.), *Numerical Dating in Stratigraphy* : Wiley, 1982,pp. 123-149.
12. Fuhrmann, U.; Lippolt, H. J.; Hess, J. C. Examination of some proposed K-Ar standards: $^{40}Ar/^{39}Ar$ analyses and conventional K-Ar dating. *Chem. Geol.* **1987**, *66*, 41–51.
13. Yoder, H. S.; Tilley, C. E. Origin of basalt magmas: an experimental study of natural and synthetic rock system. *J. Petrol.* **1962**, *3*, 346-532.
14. Xu Y. G.; Bodinier J. L. Contrasting enrichments in high and low temperature xenoliths from Nushan, Eastern China: Results of a single metasomatic event during lithospheric accretion? *J. Petrol.* **2004,** *45*, 321-341.
15. Hofmann, A.W. Chemical differentiation of the Earth: the relationship between mantle continental crust and oceanic crust. *Earth Planet. Sci. Lett.* **1988**,*79*, 270–280.
16. Sun, S. S.; McDonough, W. F. Chemical and isotopic systematics of oceanic basalts: implications for mantle composition and processes. *J Geol. Soc. London Spec. Publ.* **1989**, *42*,313-345.
17. Zou, H.; Zindler, A.; Xu, X.; Qi, Q. Major, trace element, and Nd, Sr and Pb isotope studies of Cenozoic basalts in SE China: mantle sources, regional variations, and tectonic significance. *Chem. Geol.* **2000**, *171*, 33-47.
18. Li, Z. X. Collision between the North and South China blocks: a crustal-detachment model for suturing in the region east of the Tanlu fault. *Geology* **1994**, *22*, 739-742.
19. Meng, F.; Gao, S.; Niu, Y.; Liu, Y.; Wang, X. Mesozoic–Cenozoic mantle evolution beneath the North China Craton: A new perspective from Hf–Nd isotopes of basalts. *Gondwana Res.* **2015**, *27*, 1574–1585.
20. Chen, D. G.; Chou, H. T.; Yang, C. T.; Wang, Y. S. Petrogenesis of Cenozoic volcanic rocks and isotopic characteristics of mantle sources in Shandong, Anhwei and Jiangsu provinces. The Characteristics and dynamics of upper mantle of China. *The Seismic Press, Beijing*,1990, 124-131 (in Chinese).
21. Chen, D.; Peng, Z. K-Ar ages and Pb, Sr isotopic characteristics of some Cenozoic volcanic rocks from Anhui and Jiangsu provinces, China. *Acta Petrol. Sin.* **1988**, *2*, 3–12 (in Chinese with English abstract).
22. Liu, Y.S.; Gao, S.; Kelemen, P.B.; Xu, W.L. Recycled crust controls contrasting source compositions of Mesozoic and Cenozoic basalts in the North China Craton. *Geochim. Cosmochim. Acta* **2008**, *72*, 2349–2376.

23. Chen, L.H.; Zeng, G.; Jiang, S.Y.; Hofmann, A.W.; Xu, X.S. Sources of Anfengshan basalts: subducted lower crust in the Sulu UHP belt, China. *Earth Planet. Sci. Lett.* **2009**, *286*, 426–435.
24. Zeng, G.; Chen, L.H.; Xu, X.S.; Jiang, S.Y.; Hofmann, A.W. Carbonated mantle sources for Cenozoic intra-plate alkaline basalts in Shandong, North China. *Chem. Geol.* **2010**, *273*, 35–45.
25. Kuang, Y.S., Wei, X., Hong, L.B., Ma, J.L., Pang, C.J., Zhong, Y.T., Xu, Y.G., 2012. Petrogenetic evaluation of the Laohutai basalts from North China Craton: melting of a two-component source during lithospheric thinning in the late Cretaceous-early Cenozoic. *Lithos* **2012**, *154*, 68-82.
26. Xu, Y.G.; Zhang, H.H.; Qiu, H.N.; Ge, W.C.; Wu, F.-Y. Oceanic crust components in continental basalts from Shuangliao, Northeast China: derived from the mantle transition zone? *Chem. Geol.* **2012**, *328*, 168–184.
27. Xu, Z.; Zhao, Z.F.; Zheng, Y.F. Slab-mantle interaction for thinning of cratonic lithosphericmantle in North China: geochemical evidence from Cenozoic continental basalts in central Shandong. *Lithos* **2012**, 146, 202–217.
28. Li, H.Y.; Xu, Y.G.; Ryan, J.G.; Huang, X.L.; Ren, Z.Y.; Guo, H.; Ning, Z.G. Olivine and melt inclusion chemical constraints on the source of intracontinental basalts from the eastern North China Craton: discrimination of contributions from the subducted Pacific slab. *Geochim. Cosmochim. Acta* **2016**, *178*, 1–19.
29. Huang, X.L.; Zhong, J.W.; Xu, Y.G. Two tales of the continental lithospheric mantle prior to the destruction of the North China Craton: insights from Early Cretaceous mafic intrusions in western Shandong, East China. *Geochem. Cosmochim. Acta* **2012**, 96, 193-214.
30. Zhao, D.; Tian, Y.; Lei, J.; Liu, L.; Zheng, S. Seismic image and origin of the Changbai intraplate volcano in East Asia: Role of big mantle wedge above the stagnant Pacific slab. *Phys. Earth Planet. Inter.* **2009**, *173*, 197-206.
31. Kuritani, T.; Ohtani, E.; Kimura, J.I. Intensive hydration of the mantle transition zone beneath China caused by ancient slab stagnation. *Nat. Geosci.* **2011**, *4 (10)*,713-716.
32. Xu, Y.G. Recycled oceanic crust in the source of 90-40Ma basalts in North and Northeast China: evidence, provenance and significance. *Geochem. Cosmochim. Acta* **2014**, *143*, 49-67.
33. Li, H.Y.; Zhou, Z.; Ryan, J.G.; Wei, G.J.; Xu, Y.G. Boron isotopes reveal multiple metasomatic events in the mantle beneath the eastern North China Craton. *Geochem. Cosmochim. Acta* **2016**, *194*, 77-90.
34. Wallace, M. E.; Green, D. H. The effect of bulk compositions on the stability of amphibole in the upper mantle: implications for solidus positions and mantle metasomatism. *Mineral Petrol.* **1991**, *44*, 1-9.
35. Xu, Y. G.; Menzies, M. A.; Vroon, P.; Mercier, J. C. C.; Lin, C. Y. Texture-temperature-geochemistry relationship in the upper mantle as revealed from spinel peridotite xenoliths from Wangqing, NE China. *J. Petrol.* **1998**, *39*, 469-493.
36. Philpotts, J. A.; Schnetzler, C. C. Partition coefficients of rare-earth elements between igneous matrix material and rock-forming mineral phenocrysts—II. *Geochem. Cosmochim. Acta* **1970**, *34*, 331-340.
37. Xu, X. S.; O'Reilly, S. Y.; Griffin, W. L.; Zhou, X. M. The nature of the Cenozoic lithosphere at Nushan, Central Eastern China. In: Flower, M.; Chung, S. L.; Lo, C. H.; Lee, T. Y. (eds) Mantle Dynamics and Plate Interactions in East Asia. *A. G. U. Geodynamic Series* **1998**, *27*, 167-195.
38. Xu, Z.; Zheng, Y. F.; Zhao, Z. F. The origin of Cenozoic continental basalts in east-central China: Constrained by linking Pb isotopes to other geochemical variables. *Lithos* **2017**, *268*, 302-319.
39. Wang, Y.; Meng, X.; He, Y.; Huang, J.; Lu, W. N.; Shi, Q.; Ke, S.; Tang, Y. J.; Huang, S.; Li, S. Light calcium isotope anomaly observed in continental basaltic lavas: A mixed signal of recycled carbonate and fractionation during melting. *Lithos* **2023**, *456*, 107306-107320.
40. Dupuy, C.; Liotard, J. M.; Dostal, J. Zr/Hf fractionation in intraplate basaltic rocks: carbonate metasomatism in the mantle source. *Geochim. Cosmochim. Acta* **1992**, *56*, 2417-2423.
41. Furman, T. Melting of metasomatized subcontinental lithosphere: undersaturated mafic lavas from Rungwe, Tanzania. *Contrib. Mineral. Petrol.* **1995**, *112*, 97-115.
42. Yaxley, G. M.; Crawford, A. J.; Green, D. H. Evidence for carbonatite metasomatism in spinel peridotite xenolith from Western Victoria. *Earth Planet. Sci. Letters.* **1991**, *107*, 305-317.
43. Guo, F.; Fan, W.; Wang, Y.; Lin, G. Geochemistry of late Mesozoic mafic magmatism in west Shandong Province, eastern China: Characterizing the lost lithospheric mantle beneath the North China Block. *Geochem. J.* **2003**, *37*, 63-77.
44. Lee, Y. T.; Chen, J. C.; Shih, J. Y.; Juang, W. S.; Yang, H. R.; Huang, S. W.; Lin M. L. Geochemistry of Cenozoic basaltic rocks from Shandong province and its implication for mantle process in North China. *Geochem. J.* **2006**, *40*, 579-596.
45. Lee, Y. T.; Chen, J. C.; Shih, J. Y.; Ho, K. S.; Yang, H. R.; Lin, M. L.; Hu, Y. T.; Chiu, C. H. Petrogenesis of Cenozoic basaltic rocks from Jiangsu province, China evidence from geochemical constraints. *Acta Geol. Sinica* **2013**, *87*, 102–117.
46. Sato, H. (1977) Nickel content of basaltic magma: identifyication of primary magmas and a measure of the degree of olivine fractionation. *Lithos* **1977**, *10*, 113-120.

 doi:10.20944/preprints202311.0972.v1

47. Wilkinson, J. F. G.; Le Maitre, R. W. Upper mantle amphiboles and micas and TiO_2, K_2O, and P_2O_5 abundances and 100Mg/(Mg+Fe^{+2}) ratios of common basalts and andesites: implications for modal mantle metasomatism and undepleted mantle compositions. *J. Petrol.* **1987**, *28*, 37-73.
48. Frey, F. A.; Prinz, M. Ultramafic inclusions from San Carlos, Arizona: petrological and geochemical data bearing on their petrogenesis. *Earth Planet. Sci. Lett.* **1978**, *38*, 129-176.
49. Shaw, D. M. Trace element fractionation during anatexis. *Geochim. Cosmochim. Acta* **1970**, *34*, 237-243.
50. Brook, C. K.; Nielsen, T. F. D. The East Greenland continental margin: a transition between oceanic and continental magmatasm. *J. Geol. Soc. London* **1982**, *39*, 265-275.